Trends in Immunotherapy (2024) Volume 8 Issue 1
doi: 10.24294/ti.v8.i1.4674

ORIGINAL RESEARCH ARTICLE

The hyperplasia of the mammary gland effect of the Mongolian Remedy RuXian-I in rats reduced by estrogen and progesterone via inhibition of MAPK and NF-κB pathways

Shuangquan Zhao[1,2], Chimedragchaa Chimedtseren[1], Jambaldorj Jamiyansuren[1], Alimaa Tugjamba[1,*], Bin Zhang[2]

[1] *Mongolian National University of Medical Sciences, Ulaanbaatar 14201, Mongolia*

[2] *Affiliated Hospital of Inner Mongolia Minzu University, Tongliao 028043, China*

*** Corresponding author:** Alimaa Tugjamba, alimaa.t@mnums.edu.mn

ABSTRACT

Background: The aim of the present study was to evaluate whether the HMG (Hyperplasia of the Mammary Gland) effect of RuXian-I in estrogen- and progestogen- induced HMG rats is mediated through the activation of MAPK (Mitogen activated protein kinase) and NF-κB signaling pathways. **Materials and methods:** Fifty virgin female Wistar rats were randomly divided into ~~in~~ control and HMG, RuXian-I (0.75 $g \cdot kg^{-1}$, 1.5 $g \cdot kg^{-1}$, 3 $g \cdot kg^{-1}$, respectively) groups, 10 in each. Injections of estrogen and progestogen were given to establish rat models of HMG and RuXian-I at the same time. Changes in nipple heights were measured; pathologic changes of HMG in rats were also observed under a light microscope; the phosphorylation levels of MAPK and NF κB and the expression levels of TNF-α and IL-1β were measured. **Results:** Compared with the control group, the nipple diameters and height were increased significantly, the numbers of MG lobules were increased, there were changes in breast histopathology, the levels of TNF-α and IL-1β increased significantly, and MAPK and NF-κB were activated in HMG rats. Compared with the HMG model group, the increased nipple height was decreased, the numbers of MG lobules were reduced, the degree of HMG in rats was alleviated obviously, and the phosphorylation level of MAPK and NF-κB and cytokines TNF- α and IL-1β levels in serum were decreased by RuXian-I treatment. **Conclusion:** Those results suggest RuXian-I has protective and therapeutic effects on HMG rats induced by estrogen and progestogen and is likely to activate MAPK and NF-κB signaling pathways.

Keywords: RuXian-I; Anti-hyperplasia of mammary gland; NF-κB signaling pathways

ARTICLE INFO

Received: 18 February 2024
Accepted: 12 March 2024
Available online: 29 April 2024

1. Introduction

Hyperplasia of mammary gland (HMG) is a common breast disease in the middle-aged women all over the word and a precancerous lesion of mammary gland (MG)[1]. HMG has severe mammary cancerous tendencies, has been possibly mixed and cover with early breast cancer, and its treatment has become a research hotspot. The morbidity is enhancing quickly, with much higher risk of causing mammary carcinoma[2,3]. To date, two treatment methods of HMG, chemical agents, including estrogen therapy[4,5], and surgical excision[6], have been concerned. However, new alternative and complementary treatments are required due to their undesirable side effects, low cure rate, and high recurrence rate. Much research has proved that Traditional Chinese Medicine could improve the regulatory mechanism in the body to inhibit the HMG[7–10], especially Mongolian medicine plays an important role in treating diseases[11].

The traditional Mongolian medicine RuXian-I provided by the

Affiliated Hospital of Inner Mongolia University for Nationalities is an empirical formula specifically to use for the treatment of HMG in clinical based on the principles of traditional Mongolian medicine. RuXian-I is composed of 30 ingredients, which are Herba Leonuri Japonici, Fructus Amomi Rotundus, Flos Caryophylli, Fructus Gardeniae, Rhizoma Gymnadeniae Conopseae, Semen Myristicae, Cornu Cervi Pantotrichum, Cordyceps and so on[12]. These herbs themselves have a variety of biological activities, including anti-allergic[13], antioxidant[14] and anti-tumor[15], anti-inflammation[16] activity. RuXian-I was used to treat thousands of patients with HMG in our hospital and the cure rate was 98%. Although there is a good effect, little is known about the mechanism.

HMG takes place through the activation of multiple intracellular signaling pathways involved in inflammation reaction[17,18]. Among the existing signaling pathways, mitogen-activated protein kinase (MAPK) and nuclear factor kappa-light-chain-enhancer of activated B cells (NF-κB) signaling pathways are key regulators of the inflammatory processes[19,20]. The MAPK families are activated in response to various extracellular stimuli and regulate essential cellular events[18]. The activation through phosphorylation of three major MAPK (p38, ERK1/2 and JNK) has been shown to promote inflammatory gene expression in macrophages, thus controlling different steps in the pro-inflammatory cytokine production process[21,22]. NF-κB is a ubiquitous nuclear transcription factor that plays a major role in the regulation of many genes that encode for mediators of immune and inflammatory responses[23]. Activation of several key proteins of MAPK and NF-κB signaling pathways initiates the transcription of numerous genes, including inflammatory factors, such as the expression of tumor necrosis factor (TNF)-α, IL-1β and IL-6[24,25], and has been associated with the development of multiple types of diseases such as breast cancer, multiple myeloma, neuroblastoma[26–28]. HMG is also involved in the inflammatory process[17,18]. Therefore, in this study, to clarify whether MAPK and NF-κB signaling pathway are activated by estrogen and progestogen and whether RuXian-I can inhibit the key proteins of these two pathways and inhibit the inflammatory response in HMG.

In brief, the anti-HMG effects of RuXian-I in estrogen combined with progestogen induced HMG rats was evaluated. Acute and long-term toxicity, anti-inflammatory activity, changes of the nipple height and diameter, pathologic changes of HMG in rats, the phosphorylation level of MAPK and NF-κB and the expression levels of TNF-α and IL-1β were performed.

2. Materials and methods

2.1. Animals

Virgin female Wistar rats weighing 180–220 g for drug treatment and acute toxicity test (90 rats) and 100–140 g for long-term toxicity test (50 rats) and Kunming female mice weighing 18–22 g (60 mice) for granuloma test were supplied by Experimental Animal Center of Jilin University. The rats were raised in a quiet, temperature- and humidity-controlled room (20–25 °C and 50–60%, respectively) with a 12 h light/dark cycle and provided with rodent chow and water ad libitum, adaptively to a week before use. We compared survival in all groups throughout the treatment. All animals were carefully monitored, and the number of dead rats was recorded every day.

2.2. Toxicities of RuXian-I in rat

2.2.1. Acute toxicity

Forty rats were randomly assigned into 2 groups (n = 20). Rats were respectively administered with normal saline (20 mL·kg^{-1}, i.g.) in the control group and RuXian-I (16.32 g·kg^{-1}, i.g. the maximum allowable concentration of 40.8% of the test, the Mongolian Medicine Manufacturing Room of the Affiliated Hospital of Mongolia University for Nationalities) in administration group twice daily for 14 days. During the experiment, whether the toxic reaction and animal deaths were observed for 14 consecutive days.

2.2.2. Long-term toxicity

Four groups (n = 30) of rats weighing 100–140 g were designed, one control group, three dose groups of RuXian-I (0.75 g·kg^{-1}, 1.5 g·kg^{-1}, 3 g·kg^{-1}, respectively, i.g.). Each group of rats was administered once a day for 6 days and stopped for 1 day for 26 weeks. The control group was given the same volume of normal saline. During the trial period, the appearance, behavior, body weight, food intake, hematology and blood biochemistry of the rats were measured regularly. The main organs of the high dose group and the control group were subjected to histopathological examination at the end of the 13th week, the end of the 26th week and the 3rd week after the withdrawal, respectively.

2.3. Anti-inflammatory effects

2.3.1. Cotton pellet induced granuloma

Sixty mice were anesthetized by ether. Sterile cotton pellets (5 ± 0.5 mg, penicillin infiltration sterilization drying) were implanted in the mice bilateral axillary subcutaneous, and then sutured. Then according to body weight, mice were divided into 5 groups, the control group, the aspirin group, and the RuXian-I low, medium and high dose group. The animals received aspirin (300 mg·kg^{-1}), RuXian-I (0.75 g·kg^{-1}, 1.5 g·kg^{-1}, 3 g·kg^{-1}, respectively), once a day through an oral cannula over 15 consecutive days. The control group was given the same volume of distilled water. On the 15th day, the mice were sacrificed, and the cotton pellet were taken out and dried in an oven at 80 ℃ for 6 h and weighed. The increase in weight of cotton pellet ($W_{granuloma}$) was determined and used for further calculation. W_{body} was the weight of mice.

$$\text{Granuloma index (mg)} = W_{granuloma} / (W_{body} \times 10)$$

$$\text{Granuloma Inhibition rate (\%)} = (W_{granuloma\ (control)} - W_{granuloma\ (treatment)}) / W_{granuloma\ (control)} \times 100\%$$

2.3.2. Croton oil causes air cysts

Each group of rats was anesthetized by ether, poured into 20 mL of air in the back of the scapular sc, then injected 1% croton oil (1 mL) into the airbag, and immediately turned the back of the rat slowly down to croton oil and capsule tissue in full contact. The gas inside the capsule was pumped after 24 hours. Sixty rats were randomly divided into 5 groups (n = 10), the control group, aspirin 210 mg·kg^{-1}, RuXian-I (0.75 g·kg^{-1}, 1.5 g·kg^{-1}, 3 g·kg^{-1}, respectively), once a day through an oral cannula over 10 consecutive days. The control group was given the same volume of distilled water. The rats were sacrificed 24 h after the last administration. Intracapsular exudate was measured, and the hyperplastic granulation tissue is stripped, washed thoroughly in physiological saline, dried in an oven at 80 ℃, and weighed.

2.4. Animal model and drug treatments

The rats were randomly assigned into 5 groups (n = 10). Ten rats as normal control group were administered with olive oil (Sigma-Aldrich) intramuscularly (0.25 mL·kg^{-1}) for 30 days, and rats in the other were administered with Estradiol Benzoate (Hangzhou Animal Medicine Factory) intramuscularly (0.5 mg·kg^{-1}) for 25 days and followed with Progesterone intramuscularly (5 mg·kg^{-1}, Zhejiang Xianju Pharmaceutical Co. Ltd) for 5 days. Then, rats in normal control group and HMG control group were received normal saline (10 mL·kg^{-1}, i.g.) for 30 days, while rats in low-dosage, middle-dosage and high-dosage treatment group were treated with RuXian-I (0.75 g·kg^{-1}, 1.5 g·kg^{-1}, 3 g·kg^{-1}, respectively, i.g.) for 30 days. During the experiment, the rats' second pair of the left and right nipple diameters and height was measured until termination.

2.5. Histopathology observation

Tissues of the right MG on the right side between the second and third nipples from all groups were separated and fixed in 4% paraformaldehyde, embedded in paraffin, sectioned into 4 μm pieces, stained with Haematoxylin-Eosin (H&E), observed under light microscopy, took photos and analyzed.

2.6. Protein fraction

The tissue samples from mammary tissues (100 mg, n = 6 per group) were ground in liquid nitrogen. Whole-tissue protein fractions were repeatedly obtained by with 4 ℃ precooling RIPA Lysis buffer (Pierce, Rockford, IL, USA) for ice bath supplemented with protease inhibitor cocktail and phosphoric acid protease inhibitor cocktail (Roche, Indianapolis, IN, USA) on ice bath, and placed for 1 h, 12,000 rpm, centrifugation of 10 min at 4 ℃. Nuclear and cytoplasmic protein from mammary tissues were obtained by homogenization in cytoplasmic buffer and determined using BCA protein assay kit (Beijing Tiangen Biotech Co. Ltd).

2.7. Western blotting

Twenty micrograms of protein were electrophoresed in a 10% SDS-PAGE gel and transferred onto a PVDF membrane (Bio-Rad, Hercules, CA, USA). Extracellular signal-regulated kinase (ERK), phosphor (p)-ERK, p38, p-p38, stress-activated protein kinase (SAPK)/c-Jun N-terminal kinase (SAPK/JNK), p-SAPK/JNK, nuclear factor (NF)-κB， p-NF-κB, IκB, p-IκB and β-actin (diluted 1:1000 in 3% bovine serum albumin (BSA); Cell Signaling, USA) was then added to the membrane. Anti-rabbit alkaline phosphatase-conjugated secondary antibody (diluted 1:2000 in 3% BSA; Santa Cruz, CA, USA) was used to detect the target proteins. After incubation for 2 h at room temperature, bound antibodies were visualized using an enhanced chemiluminescence (ECL) detection reagent (Amersham Pharmacia, Piscataway, NJ, USA). Relative band densities were determined using a computerized densitometry system.

2.8. ELISA

After termination, the rats were euthanized 1 h after the last drugs administration, and the blood samples were collected from abdominal aortic. The serum samples were obtained by centrifuge at 3500 rpm for 10 min after coagulated in 4 ℃ overnight. The serum samples were used for the determination of the levels of sex hormone and stored at −80 ℃ until biochemical assays were performed. Rat serum cytokine concentrations were quantified using a mouse tumor necrosis factor (TNF)-α, interleukin (IL)-1β ELISA kit (BD Bioscience, San Jose, CA, USA) according to the instruction of ELISA test kits.

2.9. Ethical approval

This study has been approved by the Institutional Ethics Committee of Ethics Committee of Affiiated hospital of Inner Mongolla Universlty for The Nationalities Appraval Noticeand (NM-LL-2018-12-18-04) and has followed the principles outlined in the Declaration of Helsinki.

2.10. Statistical analysis

All values were expressed as the means ± SD. Data was analyzed using the SPSS17.0 statistical software. Data among the groups were analyzed by homogeneity test of variances expressed in forms of standard deviation. The comparison of multiple sample means was used with One-way ANOVA test. All experiments were performed at least three times. $P < 0.05$ was accepted as significant. The statistic and graphic software GraphPad Prism (Version 5, GraphPad Software, Inc. La Jolla, CA) was used for all statistical and graphic analysis.

3. Result

3.1. Toxicities

No significant acute toxicity was observed and no death within 14 days, no significant changes in serum hormone levels and in organ toxicity were found at 16.32 $g \cdot kg^{-1}$.

Rats were given intragastric administration for 26 weeks, and no significant changes in behavioral activity, appearance signs, body weight, food intake, hematology and serum biochemistry, organ location, appearance morphology, histopathological changes and delayed pathological changes were found at the dose of 0.75 $g \cdot kg^{-1}$,

1.5 g·kg^{-1}, 3 g·kg^{-1} (data not shown). The toxic dose of RuXian-I is greater than 3 g·kg^{-1}.

3.2. Effect of RuXian-I on anti-inflammatory in rats

3.2.1. Cotton pellet induced granuloma

Table 1 indicated that the 1.5 g·kg^{-1} and 3 g·kg^{-1} dose of RuXian-I exhibited a significant and doserelated inhibition of the dried weight of the cotton pellet granuloma, compared to the control group ($P < 0.01$). The inhibitory values for 0.75 g·kg^{-1}, 1.5 g·kg^{-1}, 3 g·kg^{-1} of RuXian-I were 14.34%, 22.71%, and 30.28% respectively. Aspirin inhibited granuloma tissue formation with a value of 26.29%, a lower value than that observed with the 3 g·kg^{-1} dose of RuXian-I. RuXian-I had the effect of inhibition of proliferative inflammation, but its inhibition of inflammatory hyperplasia is not as good as aspirin.

Table 1. Effect of oral administration of RuXian-I in mice cotton pellet induced inflammation.

Groups	Dosages (g·kg^{-1})	Animals	Granuloma weight (mg)	Inhibition rate (%)	*p*
Control	-	10	50.20 ± 10.49	-	
Aspirin	300 mg·kg^{-1}	10	37.00 ± 10.85	26.29	$P < 0.01$
RuXian-I	0.75	10	35.00 ± 7.15	14.34	$P > 0.05$
-	1.5	10	38.80 ± 12.21	22.71	$P < 0.05$
-	3	10	430 ± 7.76	30.28	$P < 0.01$

3.2.2. Croton oil causes air cysts

High-dosage treatment group significantly inhibited the inflammatory exudate and granulation tissue hyperplasia caused by croton oil compared with the control group ($P < 0.01$), but its anti-inflammatory effect was not as good as that of aspirin ($P < 0.01$, **Figure 1**).

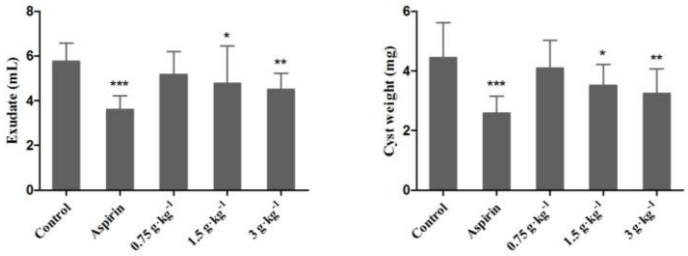

Figure 1. Effect of RuXian-I on air cysts caused by croton Oil, The inflammatory exudate and cyst weight in different groups. Values are the mean ± S.D. * $P < 0.05$, ** $P < 0.01$, *** $P < 0.001$ vs. control group.

3.3. Effect of RuXian-I on the nipple height and diameter in rats

The nipple height and diameter (left 2 and right 2) was measured at the end of the experiment. The nipple height and diameter were enlarged in HMG model group on estrogen and progestogen-inducted ($P < 0.01$ vs. control group), while this indicator showed a dose dependent alleviation in RuXian-I-treated group ($P < 0.01$ vs. HMG group, **Figure 2**).

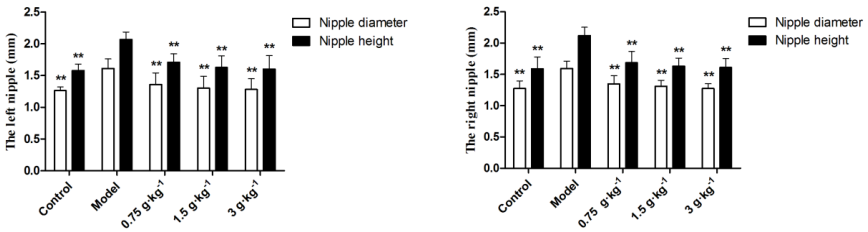

Figure 2. Effect of RuXian-I on the left and right nipple diameter and height changes at the end of the administration. Values are the mean ± S.D. * $P < 0.05$, ** $P < 0.01$, *** $P < 0.001$ vs. HMG group.

3.4. Effect of RuXian-I on MG histopathologic changes in rats

To evaluate the degree of hyperplasia in HMG rats, H&E staining was performed on MG sections in each groups. Histopathologic examination of MG in the control group showed normal histological architecture: no proliferative lesions, fewer acinars, no mammary duct secretion, no mammary duct ectasia and no expansion of mammary lumens. And there was no significant stromal hyperplasia (**Figure 3A**).

Mammary epithelial cell in HMG group irregularly arranged, histological abnormalities in model rat mammaries also showed apparently hyperplasy, lobules significantly increased and expanded, numbers of acinars increased, mammary ducts ectasia, expansion of mammary lumens. However, no mammary tumors were observed (**Figure 3B**).

In all RuXian-I treated group, the number and size of rat MG lobules and acini and cavity secretions were less than the HMG group. Catheter lumen and volume become smaller in treatment groups (**Figures 3C, 3D, 3E**). Especially in the high-dosage group, RuXian-I (3 $g \cdot kg^{-1}$) markedly alleviated the degree of HMG, mammary lobules significantly lowered, numbers of acinars decreased, no obviously mammary ducts secretion (**Figure 3E**).

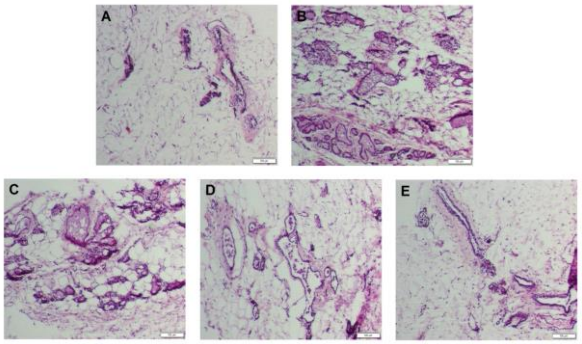

Figure 3. Histological image of MG tissue (original magnification, 400×). **(A)** control group; **(B)** HMG group; **(C)** 1.0 $g \cdot kg^{-1}$ RuXian-I group; **(D)** 1.5 $g \cdot kg^{-1}$ RuXian-I group; **(E)** 2.0 $g \cdot kg^{-1}$ RuXian-I group.

3.5. Effects of RuXian-I on NF-κB and MAPK activation in rats

To elucidate whether the inhibition of the secretion of inflmmatory mediators by RuXian-I is mediated through the activation of MAPK signaling pathways, we evaluated several key MAPK signaling molecules (ie, p38, ERK1/2, and JNK) in control group, HMG group and RuXian-I group, by western blotting studies. **Figure 4A** indicates that the estrogen and progestogen treatment induced a strong phosphorylation of ERK1/2, p38 and JNK that peaks ($p < 0.001$ vs. control group), and these were decreased by RuXian-I ($p < 0.01$). The three proteins in RuXian-I middle dose group seemed to be obviously lower than those in RuXian-I high dose group.

Following, we investigated the inhibitory effect of RuXian-I on NF-κB activation by assessing the phosphorylation level of p-IκB-α, IκB-α and p-p65 protein, by western blotting studies. As depicted in **Figure 4B**, the stimulation of rats with the estrogen and progestogen resulted in an obvious phosphorylation of IκB-α and p-p65 ($p < 0.001$ vs. control group). Comparing with the HMG group, it is evident that RuXian-I leads to a significant inhibition of p-IkB-α and p-p65 at dose of low, middle and high ($p < 0.05$), and these decreases were accompanied by dose-dependent reductions. In the case of IκB-α, HMG group was importantly decreased ($p < 0.001$ vs. control group), while RuXian-I-treated group was importantly increased ($p < 0.01$ vs. HMG group).

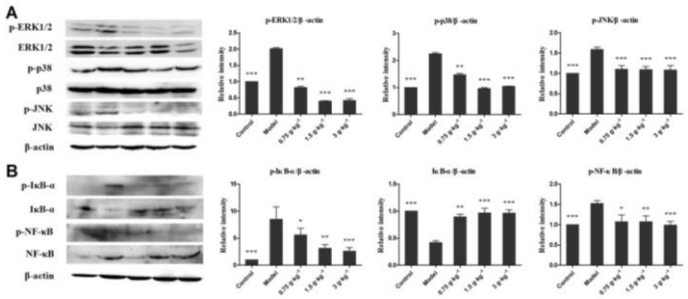

Figure 4. (A) Effect of RuXian-I on MAPK signaling pathways; (B) Effect of RuXian-I on NF-KB signaling pathways. Values are the mean ± S.D. * $P < 0.05$, ** $P < 0.01$, *** $P < 0.001$ vs. HMG group.

3.6. Effects of RuXian-I on TNF-α and IL-1β level in rats

we evaluated the levels of cytokines TNF-α and IL-1β using ELISA. Levels of TNF-α and IL-1β were increased in HMG group ($p < 0.001$ vs. control group). RuXian-I significantly reduced the level of TNF-α in a dose-dependent manner, compared to the HMG group. The level of IL-1β was decreased by RuXian-I high dosage treatment (**Figure 5**).

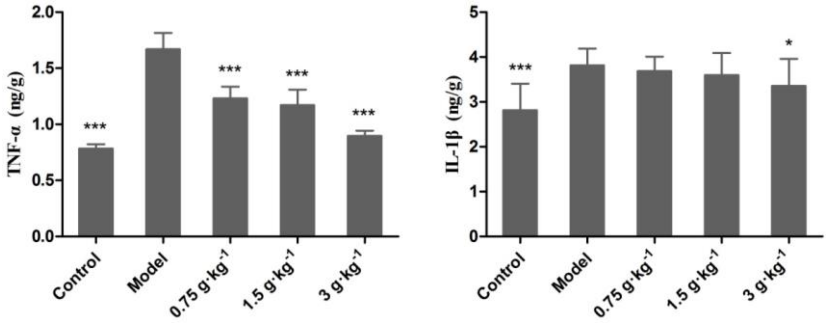

Figure 5. Effect of RuXian-I on the expression of TNF-α and IL-1β.
Values are the mean ± S.D. * $P < 0.05$, ** $P < 0.01$, *** $P < 0.001$ vs. HMG group.

4. Discussion and conclusion

Toxicity results indicate that RuXian-I has no acute toxicity at 16.32 g·kg^{-1} and long-term toxicity at the dose of 0.75 g·kg^{-1}, 1.5 g·kg^{-1}, 3 g·kg^{-1} for HMG rats induced by estrogen and progestogen. Comparing with the HMG group, the MG of group given 0.75 g·kg^{-1}, 1.5 g·kg^{-1}, 3 g·kg^{-1} RuXian-I also recovered well, the heights and diameters of nipples, lobule volumes, numbers of mammary lobules and acinars remarkably decreased in different degree.

This study provides evidence that RuXian-I acts as an anti-inflammatory agent in chronic inflammation model mice and rats. The inflammatory granuloma and inflammatory exudate are the typical feature of the established chronic inflammatory process. The cotton pellet granuloma method has been widely employed to evaluate the proliferative components of chronic inflammation, because the dried weight of the pellets is closely related to the number of granulomatous tissues[29].

Activation of MAPK and NF-κB signaling molecules plays an important role in different aspects of mammary development[30,31]. The MAPK pathway is strongly implicated in morphogenesis of branched epithelial tissues, including salivary gland[32], kidney[33], lung[34] and so on, but less is known about the role of MAPK flux in mammary morphogenesis. p38 MAPK, a key player in the inflammatory responses, is involved in stress-induced gene expression[20,35,36] and its activation has a crucial role in controlling the expression of TNF-α[37]. Similarly, ERK and JNK kinases are also known as stress-activated proteins[25,37–39]. A study revealed that modulation of MAPK by cell polarity mechanisms is required during mammary development[30]. Persistent MAPK pathway activation undermines mammary epithelial organization[40]. Our results confirm this statement, that is, the activation of p38, ERK1/2, and JNK occurred the estrogen and progestogen-treated

mammary gland, and RuXian-I significantly reduced their phosphorylated states, showing that RuXian-I exert their protective effects against inflammatory responses partly by blocking the MAPK signaling pathways.

The activation of the MAPK pathway is crucial for the subsequent activation of NF-κB signaling complex[41,42]. Aberrant NF-κB activation can lead to pre-malignant changes in the breast[31]. NF-κB is a ubiquitous nuclear transcription factor that plays a critical role in the regulation of many genes that encode for mediators of immune and inflammatory responses[23]. Under physiological conditions, NF-κB is sequestered into the cytosol by IκB protein[43]. Upon inflammatory stimuli, including TNF-α, IκB-α is phosphorylated and subsequently degraded, which enables NF-κB to migrate to the nucleus[44–47]. NF-κB then binds to its specific promoter region, and initiates the transcription of numerous genes, including inflammatory factors, such as IL-1β, IL-6, TNF-α[24]. In addition, many studies showed that the activation of NF-κB is mediated by a wide variety of upstream signals, including the MAPK (p38, ERK1/2, and JNK)[48–50] The MAPK are sensitive to stimulators that cause oxidative stress, including metal neurotoxicity[22]. In the present study, level of serum inflammatory factors, IL-1β and TNF-α, was elevated in HMG. Thus, inhibition of NF-κB signaling following acute inflammation or the initial signs of hyperplastic growth could represent an important opportunity for breast cancer prevention[31]. As already presented, pre-treatment with RuXian-I significantly increased the cytosolic level of IκB-α, while it reduced NF-κB expression in the nucleus of HMG cell. This suggested that RuXian-I inhibited NF-κB subunit translocation from the cytoplasm to the nucleus and thereby inhibited the DNA binding activity of NF-κB in MG cell, suggesting that RuXian-I impedes NF-κB activation in HMG cell. In summary, the Ruxi-I therapeutic mechanism first inhibits MAPK signaling pathway, then inhibits NF-κB, and then reduces the release of inflammatory cytokines TNF-α and IκB-α, thereby reducing the inflammatory response of HMG.

This paper provides evidence that RuXian-I acts as anti-inflammatory agent in HMG model rats and has protective and therapeutic effects on HMG rats by blocking the MAPK and NF-κB signaling pathways and adjusting secretion of TNF-α and IL-1β. This paper provides a strong theoretical basis for basic research on the potential drug Ruxi-I in clinical treatment of HMG. Ruxi-i may bring good news to HMG patients all over the world in the future.

There are also some limitations in this study: First, the development process of HMG is complex, and the evolution process of its mechanism cannot be better explained. Second, Ruxi-I is composed of a variety of Chinese herbs and has a variety of pharmacological effects, and it is unclear whether there are other mechanisms that can shield HMG. Third, our experimental model was female rats, and clinical HMG patients were both male and female, mainly middle-aged women. Therefore, our findings may just provide some hints for the treatment of female clinical patients.

Author contributions

Conceptualization, SZ; methodology, JJ; software, AT; resources, CC; data curation, AT; writing—original draft preparation, JJ; writing—review and editing, BZ. All authors have read and agreed to the published version of the manuscript.

Conflict of interest

The authors declare no conflict of interest.

References

1. Weaver M, Stuckey A. Benign Breast Disorders. Obstetrics and Gynecology Clinics of North America. 2022; 49(1): 57-72. doi: 10.1016/j.ogc.2021.11.003
2. Wang L, Zhao D, Di L, et al. The anti-hyperplasia of mammary gland effect of Thladiantha dubia root ethanol extract in rats reduced by estrogen and progestogen. Journal of Ethnopharmacology. 2011; 134(1): 136-140. doi: 10.1016/j.jep.2010.11.071

3. Zhang G, Li D, Guo H, et al. Modulation of expression of p16 and her2 in rat breast tissues of mammary hyperplasia model by external use of rupifang extract. Journal of Traditional Chinese Medicine. 2012; 32: 651-656.
4. Fan P, Maximov PY, Curpan RF, et al. The molecular, cellular and clinical consequences of targeting the estrogen receptor following estrogen deprivation therapy. Molecular and Cellular Endocrinology. 2015; 418: 245-263. doi: 10.1016/j.mce.2015.06.004
5. Jordan VC. The new biology of estrogen-induced apoptosis applied to treat and prevent breast cancer. Endocrine-Related Cancer. 2014; 22(1): R1-R31. doi: 10.1530/erc-14-0448
6. Nguyen CV, Albarracin CT, Whitman GJ, et al. Atypical Ductal Hyperplasia in Directional Vacuum-Assisted Biopsy of Breast Microcalcifications: Considerations for Surgical Excision. Annals of Surgical Oncology. 2010; 18(3): 752-761. doi: 10.1245/s10434-010-1127-8
7. Feng S, Han M, Lai L, et al. Research Capacity at Traditional Chinese Medicine (TCM) Centers in China: A Survey of Clinical Investigators. Evidence-Based Complementary and Alternative Medicine. 2017; 2017: 1-8. doi: 10.1155/2017/4231680
8. Meng F, Li J, Wang W, et al. Gengnianchun, a Traditional Chinese Medicine, Enhances Oxidative Stress Resistance and Lifespan in Caenorhabditis elegans by Modulating daf-16/FOXO. Evidence-Based Complementary and Alternative Medicine. 2017; 2017: 1-10. doi: 10.1155/2017/8432306
9. Wang Y, Zhang Y, Jiang R. Early traditional Chinese medicine bundle therapy for the prevention of sepsis acute gastrointestinal injury in elderly patients with severe sepsis. Scientific Reports. 2017; 7(1). doi: 10.1038/srep46015
10. Du C, Li Z, Wang S, et al. Tongshu Capsule Down-Regulates the Expression of Estrogen Receptor α and Suppresses Human Breast Cancer Cell Proliferation. Kang T, ed. PLoS ONE. 2014; 9(8): e104261. doi: 10.1371/journal.pone.0104261
11. Oyunchimeg B, Hwang JH, Ahmed M, et al. Complementary and alternative medicine use among patients with cancer in Mongolia: a National hospital survey. BMC Complementary and Alternative Medicine. 2017; 17(1). doi: 10.1186/s12906-017-1576-8
12. Wang ZC, E D, Batu DL, et al. 2D-DIGE Proteomic Analysis of Changes in Estrogen/Progesterone-Induced Rat Breast Hyperplasia upon Treatment with the Mongolian Remedy RuXian-I. Molecules. 2011; 16(4): 3048-3065. doi: 10.3390/molecules16043048
13. Wu TF, Chan YY, Shi WY, et al. Uncovering the Molecular Mechanism of Anti-Allergic Activity of Silkworm Pupa-Grown Cordyceps militaris Fruit Body. The American Journal of Chinese Medicine. 2017; 45(03): 497-513. doi: 10.1142/s0192415x17500306
14. Xiao Y, Huang Q, Zheng Z, et al. Construction of a Cordyceps sinensis exopolysaccharide-conjugated selenium nanoparticles and enhancement of their antioxidant activities. International Journal of Biological Macromolecules. 2017; 99: 483-491. doi: 10.1016/j.ijbiomac.2017.03.016
15. Liu F, Zhu ZY, Sun X, et al. The preparation of three selenium-containing Cordyceps militaris polysaccharides: Characterization and anti-tumor activities. International Journal of Biological Macromolecules. 2017; 99: 196-204. doi: 10.1016/j.ijbiomac.2017.02.064
16. Lin WH, Kuo HH, Ho LH, et al. Peanut root extracts and resveratrol inhibit lipopolysaccharide-induced inflammation by suppression of mapks signaling pathways in BV-2 cells. Indian Journal of Agricultural Research. 2014; 48(1): 16. doi: 10.5958/j.0976-058x.48.1.003
17. Holloway RW, Bogachev O, Bharadwaj AG, et al. Stromal Adipocyte Enhancer-binding Protein (AEBP1) Promotes Mammary Epithelial Cell Hyperplasia via Proinflammatory and Hedgehog Signaling. Journal of Biological Chemistry. 2012; 287(46): 39171-39181. doi: 10.1074/jbc.m112.404293
18. Foote MR, Giesy SL, Bernal-Santos G, et al. t10,c12-CLA decreases adiposity in peripubertal mice without dose-related detrimental effects on mammary development, inflammation status, and metabolism. American Journal of Physiology-Regulatory, Integrative and Comparative Physiology. 2010; 299(6): R1521-R1528. doi: 10.1152/ajpregu.00445.2010
19. Ding Y, Chen Q. The NF-κB Pathway: a Focus on Inflammatory Responses in Spinal Cord Injury. Molecular Neurobiology. 2023; 60(9): 5292-5308. doi: 10.1007/s12035-023-03411-x
20. Yang Y, Kim SC, Yu T, et al. Functional Roles of p38 Mitogen-Activated Protein Kinase in Macrophage-Mediated Inflammatory Responses. Mediators of Inflammation. 2014; 2014: 1-13. doi: 10.1155/2014/352371
21. Seo J, Lee U, Seo S, et al. Anti-inflammatory and antioxidant activities of methanol extract of Piper betle Linn. (Piper betle L.) leaves and stems by inhibiting NF-κB/MAPK/Nrf2 signaling pathways in RAW 264.7 macrophages. Biomedicine & Pharmacotherapy. 2022; 155: 113734. doi: 10.1016/j.biopha.2022.113734
22. kodi T, Sankhe R, Gopinathan A, et al. New Insights on NLRP3 Inflammasome: Mechanisms of Activation, Inhibition, and Epigenetic Regulation. Journal of Neuroimmune Pharmacology. 2024; 19(1). doi: 10.1007/s11481-024-10101-5
23. Peng S, Shen L, Yu X, et al. The role of Nrf2 in the pathogenesis and treatment of ulcerative colitis. Frontiers in Immunology. 2023; 14. doi: 10.3389/fimmu.2023.1200111
24. Hatala P, Sebők C, Mackei M, et al. Molecular effects of intermittent stress on primary feline uroepithelial cell culture as an in vitro model of feline idiopathic cystitis. Frontiers in Veterinary Science. 2023; 10. doi: 10.3389/fvets.2023.1258375

25. Abdyeva A, Kurtova E, Savinkova I, et al. Long-Term Exposure of Cultured Astrocytes to High Glucose Impact on Their LPS-Induced Activation. International Journal of Molecular Sciences. 2024; 25(2): 1122. doi: 10.3390/ijms25021122
26. Stewart BJ, Fergie M, Young MD, et al. Spatial and molecular profiling of the mononuclear phagocyte network in classic Hodgkin lymphoma. Blood. 2023; 141: 2343-2358.
27. Joshi DM, Pathak SS, Banmare S, et al. Review of Phytochemicals Present in Psidium guajava Plant and Its Mechanism of Action on Medicinal Activities. Cureus. 2023; 15: e46364.
28. Cui Z wen, Xie Z xing, Wang B feng, et al. Carvacrol protects neuroblastoma SH-SY5Y cells against Fe2+-induced apoptosis by suppressing activation of MAPK/JNK-NF-κB signaling pathway. Acta Pharmacologica Sinica. 2015; 36(12): 1426-1436. doi: 10.1038/aps.2015.90
29. Che Sulaiman IS, Mohamad A, Ahmed OH. Murdannia loriformis: A Review of Ethnomedicinal Uses, Phytochemistry, Pharmacology, Contemporary Application, and Toxicology. Arcanjo DDR, ed. Evidence-Based Complementary and Alternative Medicine. 2021; 2021: 1-15. doi: 10.1155/2021/9976202
30. Godde NJ, Sheridan JM, Smith LK, et al. Scribble Modulates the MAPK/Fra1 Pathway to Disrupt Luminal and Ductal Integrity and Suppress Tumour Formation in the Mammary Gland. Hunter KW, ed. PLoS Genetics. 2014; 10(5): e1004323. doi: 10.1371/journal.pgen.1004323
31. Barham W, Chen L, Tikhomirov O, et al. Aberrant activation of NF-κB signaling in mammary epithelium leads to abnormal growth and ductal carcinoma in situ. BMC Cancer. 2015; 15(1). doi: 10.1186/s12885-015-1652-8
32. Menon RT, Thapa S, Shrestha AK, et al. Extracellular Signal-Regulated Kinase 1 Alone Is Dispensable for Hyperoxia-Mediated Alveolar and Pulmonary Vascular Simplification in Neonatal Mice. Antioxidants. 2022; 11(6): 1130. doi: 10.3390/antiox11061130
33. Mol P, Balaya RDA, Dagamajalu S, et al. A network map of GDNF/RET signaling pathway in physiological and pathological conditions. Journal of Cell Communication and Signaling. 2023; 17(3): 1089-1095. doi: 10.1007/s12079-023-00726-1
34. Tang N, Marshall WF, McMahon M, et al. Control of Mitotic Spindle Angle by the RAS-Regulated ERK1/2 Pathway Determines Lung Tube Shape. Science. 2011; 333(6040): 342-345. doi: 10.1126/science.1204831
35. Morales-Martínez M, Vega MI. p38 Molecular Targeting for Next-Generation Multiple Myeloma Therapy. Cancers. 2024; 16(2): 256. doi: 10.3390/cancers16020256
36. Shnayder NA, Ashkhotov AV, Trefilova VV, et al. Molecular Basic of Pharmacotherapy of Cytokine Imbalance as a Component of Intervertebral Disc Degeneration Treatment. International Journal of Molecular Sciences. 2023; 24(9): 7692. doi: 10.3390/ijms24097692
37. Jang HJ, Kim KH, Park EJ, et al. Anti-Inflammatory Activity of Diterpenoids fromCelastrus orbiculatusin Lipopolysaccharide-Stimulated RAW264.7 Cells. Journal of Immunology Research. 2020; 2020: 1-12. doi: 10.1155/2020/7207354
38. Hashimoto R, Koide H, Katoh Y. MEK inhibitors increase the mortality rate in mice with LPS-induced inflammation through IL-12-NO signaling. Cell Death Discovery. 2023; 9(1). doi: 10.1038/s41420-023-01674-w
39. Lee HN, Choi JH, Park JY, et al. Combination of vegetable soup and glucan demonstrates synergistic effects on macrophage-mediated immune responses. Food Science and Biotechnology. 2021; 30(4): 583-588. doi: 10.1007/s10068-021-00888-x
40. Caruso M, Saberiseyedabad K, Mourao L, et al. A Decision Tree to Guide Human and Mouse Mammary Organoid Model Selection. Methods Mol Biol. 2024; 2764: 77-105.
41. Xie C, Lin X, Hu J, et al. The polysaccharide from Camellia oleifera fruit shell enhances immune responses via activating MAPKs and NF-κB signaling pathways in RAW264.7 macrophages. Food & Nutrition Research. 2022; 66. doi: 10.29219/fnr.v66.8963
42. Wu Y, Zhao Y, Guan Z, et al. JNK3 inhibitors as promising pharmaceuticals with neuroprotective properties. Cell Adhesion & Migration. 2024; 18(1): 1-11. doi: 10.1080/19336918.2024.2316576
43. Lu Y, Guo X, Xu F, et al. Protective effects of puerarin on liver tissue in Salmonella-infected chicks: a proteomic analysis. Poultry Science. 2024; 103(1): 103281. doi: 10.1016/j.psj.2023.103281
44. Li K, Yang M, Tian M, et al. The preventive effects of Lactobacillus casei 03 on Escherichia coli-induced mastitis in vitro and in vivo. Journal of Inflammation. 2024; 21(1). doi: 10.1186/s12950-024-00378-x
45. Kim JY, Jee HG, Kim JY, et al. NF-κB p65 and TCF-4 interactions are associated with LPS-stimulated IL-6 secretion of macrophages. Biochemistry and Biophysics Reports. 2024; 38: 101659. doi: 10.1016/j.bbrep.2024.101659
46. Gambirasi M, Safa A, Vruzhaj I, et al. Oral Administration of Cancer Vaccines: Challenges and Future Perspectives. Vaccines. 2023; 12(1): 26. doi: 10.3390/vaccines12010026
47. Alagan A, Jantan I, Kumolosasi E, et al. Protective Effects of Phyllanthus amarus Against Lipopolysaccharide-Induced Neuroinflammation and Cognitive Impairment in Rats. Frontiers in Pharmacology. 2019; 10. doi: 10.3389/fphar.2019.00632
48. Mendes-Oliveira J, Campos FL, Ferreira SA, et al. Endogenous GDNF Is Unable to Halt Dopaminergic Injury Triggered by Microglial Activation. Cells. 2023; 13(1): 74. doi: 10.3390/cells13010074

49. Anwar S, Khan S, Almatroudi A, et al. A review on mechanism of inhibition of advanced glycation end products formation by plant derived polyphenolic compounds. Molecular Biology Reports. 2021; 48(1): 787-805. doi: 10.1007/s11033-020-06084-0
50. Tsai YT, Kao ST, Cheng CY. Medicinal Herbs and Their Derived Ingredients Protect against Cognitive Decline in In Vivo Models of Alzheimer's Disease. International Journal of Molecular Sciences. 2022; 23(19): 11311. doi: 10.3390/ijms231911311